Solid–Solid Reaction Kinetics: Formation of Tricalcium Aluminate

Chinmay Ghoroi and A. K. Suresh
Dept. of Chemical Engineering, Indian Institute of Technology–Bombay, Powai, Mumbai 400 076, India

DOI 10.1002/aic.11086
Published online January 3, 2007 in Wiley InterScience (www.interscience.wiley.com).

Tricalcium aluminate is an important constituent of Portland cement, apart from having other applications. It is formed by a solid–solid reaction between CaO and Al_2O_3, themselves formed by solid-state decompositions of $CaCO_3$ and $Al(OH)_3$, respectively. There is no unanimity in the literature about the kinetic and mechanistic aspects of its formation. In this article we report experimental studies on this system with a view to identifying the reasons for these discrepancies and to present reproducible kinetic information under a well-defined set of conditions. The experiments cover a temperature range of 1100–1300°C and use $CaCO_3$ and $Al(OH)_3$ gel powder as the starting materials. Reactions have been carried under a variety of conditions in an attempt to identify the experimental variables that influence the observed kinetics. The results show that mechanochemical activation can profoundly influence rates. The most reproducible and consistent results were obtained under conditions of good interparticle contact, with controlled pretreatment to define the physical structure of the reacting entity. Further, the results throw light on the sequential nature of the reaction and establish the nature of the intermediate phase. The data, when interpreted in the traditional manner, show consistent trends with the literature, but the deficiencies of such interpretation have been analyzed and the need for new models has been advanced. Because solid–solid reactions are generally less well understood than their fluid counterparts, our results argue in favor of a comprehensive modeling framework for such series reaction networks in the solid phase. © 2007 American Institute of Chemical Engineers *AIChE J,* 53: 502–513, 2007

Keywords: solid–solid reactions in series, reaction kinetics, solid processing, QXRD

Introduction

In cement chemistry, tricalcium aluminate ($Ca_3Al_2O_6$) is normally denoted by C_3A ($C \equiv CaO$ and $A \equiv Al_2O_3$). C_3A is the most reactive part (~5–10%) of the Ordinary Portland Cement (OPC) clinker,[1] produced worldwide in high tonnage. When impurities such as K^+, Na^+, Si^{4+}, and Fe^{3+} are incorporated into C_3A crystals, it is called celite, which melts at about 1350°C and assists the other reactions in the rotary cement kiln.[1] During hydration of cement, it readily reacts with water and forms a stable cubic hydrate $Ca_3Al_2(OH)_{12}$,[2] which reacts with gypsum to form calcium sulfoaluminate hydrate gel, which surrounds the cement grain and delays the reaction between water and calcium silicate phases to allow for the required workability. Apart from its use as a cement phase, application of C_3A phase as a catalyst support[3] and as a doping material to improve the biocompatibility and bioactivity of calcium aluminate bone cement[4] has emerged in recent years.

C_3A is formed by a solid–solid reaction between CaO and Al_2O_3 at high temperatures. In spite of a long history of application, the kinetics of formation of C_3A has eluded consensus and studies continue. One part of the debate concerns the identity and sequence of phases that form, *en route*, the final equilibrium phase. The other concerns the kinetics of conversion. Difficulties seem to arise from the (often ill-

Correspondence concerning this article should be addressed to A. K. Suresh at aksuresh@iitb.ac.in

Table 1. A Partial List of Model Equations Used to Describe the Kinetics of Solid–Solid Reactions*

Symbol	Model (Type of Process)	Equations
D_1	One-dimensional diffusion	$\alpha^2 = kt$
D_2	Two-dimensional diffusion	$(1-\alpha)\ln(1-\alpha)+\alpha = kt$
D_3	Jander (diffusion)	$[1-(1-\alpha)^{1/3}]^2 = kt$
$D_{3'}$	Kroger and Ziegler (diffusion)	$[1-(1-\alpha)^{1/3}]^2 = k\ln t$
D_4	Ginstling–Brounshtein (diffusion)	$1-(2/3)\alpha-(1-\alpha)^{2/3} = kt$
VC	Valensi–Carter (diffusion with volume change)	$[z/(z-1)]-(1-\alpha)^{2/3} - [1+(z-1)\alpha]^{2/3}/(z-1) = kt$
F_1	First-order kinetics	$-\ln(1-\alpha) = kt$
R_3	Phase boundary reaction	$1-(1-\alpha)^{1/3} = kt$
$R_{3'}$	Phase boundary reaction	$1-(1-\alpha)^{1/3} = k\ln t$
A_2	Avrami Erofe'ev (Nucleation and growth)	$[-\ln(1-\alpha)]^{1/2} = kt$
A_3	Avrami Erofe'ev (Nucleation and growth)	$[-\ln(1-\alpha)]^{1/3} = kt$

*From Sharp et al.[15] and Tamhankar and Doraiswamy.[16]

defined) conditions of solid–solid contact under which the experimental studies are carried out and from the inadequate justification for the models normally used in data interpretation. The present study was thus undertaken to examine the possible reasons for the disagreement that exists in the literature, to obtain data to clarify these matters to the extent possible and to explore directions for the further work in this area.

Literature

Over the years, many researchers[2,5–14] have studied the formation kinetics of calcium aluminates. In cases such as this, particle level kinetics is usually represented by an equation of the form $g(\alpha) = kt$, where $g(\alpha)$ is a function of the overall conversion, α. k and t are the rate parameter and time, respectively. The form, inspired by particle-level models for gas–solid reactions, cannot be justified rigorously in all cases, but often fits the data adequately and has continued to be applied. The more commonly used forms for solid–solid reactions of this type are given in Table 1. These models differ in terms of the geometry considered, assumptions made on the underlying process, and rate controlling mechanism. Apart from expressions based on an overall reaction order, diffusion or chemical reaction control at the phase boundary and nucleation and growth control have often been tried. Sharp et al.[15] proposed a reduced time plot method for model discrimination, which involves plotting the fractional conversion against time (t), normalized with respect to time for 50% conversion, $t_{0.5}$. This normalization cancels out the rate parameter (k) and a fit or otherwise of a model can be assessed. A plot of the appropriate $g(\alpha)$ vs. t is then used to calculate the rate parameter for different temperatures. The activation energy (E) and preexponential factor (A) can be determined (assuming an Arrhenius-type formulation for the rate parameter) from plots of $\ln(k)$ vs. $1/T$.

The different models, which have been claimed to explain the formation of calcium aluminate phases, are listed in Table 2. The more prominent among the models are attributed to Jander,[21] Ginstling and Brounshtein,[22] and Carter.[23,24] Jander's model[21] treats the diffusion-controlled case in a flat slab geometry (D_3). Ginstling and Brounshtein[22] proposed a similar model (D_4) for a spherical geometry. These models use an unreacted core approach and treat the moving boundary diffusion problem (arising out of the shrinkage of the unreacted reactant layer) in a quasi-steady-state manner. Carter[23,24] proposed a modification of an earlier model proposed by Valensi,[25] which accounts for volume change of the particle with reaction (arising out of a difference in density between the reactant and product) while retaining the quasi-steady-state features to treat the boundary movements. In this [Valensi–Carter (VC)] model, volume change has been accommodated by introducing a parameter z, which is the ratio of the volume of product formed per unit volume of the reactant consumed.

Carter[23] observed that, "to warrant any conclusions as to the validity of a model, the data must fit the model to 100%." It is therefore worth noting that most of the data taken for model validation stop well short of 100% conversion. Even so, the lack of consensus in the literature on the data and interpretation of kinetics for the calcia–alumina system is clear from Table 2. This suggests that unsuspected experimental variables (which are possibly different between different experimental studies) have influenced the observed kinetics.

There are also other difficulties in expecting models of the type listed in Table 1 to work in general. One important issue is that these models consider the solid-state reaction to occur in a single step, whereas in many cases, intermediate phases have been experimentally observed in significant amounts even at moderately high conversions, indicating a reaction network of some complexity. Such is the case, for example, with calcia–alumina reactions. The work of Mohamed and Sharp[14] on tricalcium aluminate shows the intermediate phases ($C_{12}A_7$ and CA) in substantial amounts, these phases converting slowly to the final product C_3A only at longer times. The matter is further complicated by the fact that there is no general agreement on the intermediate phases that form and the sequence of their formation.

In addition to the above difficulties with the theories, there are experimental factors that could affect the observed

Table 2. Models Used for Formation of Different Calcium Aluminate Phases

Reaction System with Mole Ratio	[Ref]Model Fitted	Temperature Range (°C)	Phase Formed
$3CaO:Al_2O_3$	[8]D_4	1100–1300	C_3A
$CaCO_3:Al_2O_3$	[10]$D_{3'}$	1200–1380	CA
$CaCO_3:Al_2O_3$	[11]D_4, VC	1200–1300	CA
$3CaO:Al_2O_3$	[11]D_4, VC	1200–1300	C_3A
$CaCO_3:2Al_2O_3$	[12]$R_{3'}$	1410–1560	CA_2
$CaO:2Al_2O_3$	[13]R_3	1200–1460	CA_2
$3CaCO_3:Al_2O_3$	[14]D_4	1150–1350	C_3A
$CaCO_3:Al_2O_3$	[17]R_3, VC	1200–1400	CA
$CA:Al_2O_3$	[18]R_3	1350–1450	CA_2
$CaCO_3:Al_2O_3$	[19]D_4	1150–1400	CA
$12CaCO_3:7Al_2O_3$	[20]D_4	1150–1350	$C_{12}A_7$

kinetics, which are not always tightly controlled. Such factors include the method used to ensure a homogeneous mix, the degree of homogeneity of the mix, particle size distribution, contact between the particles, particle shape, and interaction between particles. Variation of diffusivity with composition and any effect of pretreatment are other factors whose effect is either unknown or difficult to quantify. For example, the work of Rivas Mercury et al.[2] shows that considerable mechanical activation can result from certain methods adopted for size reduction and mixing.

It is the purpose of this article to investigate the effect of some of the more important variables in the case of the calcia–alumina system. The nature and sequence of phase formation is of particular interest because this can point to the kind of models that need to be used to describe such kinetics.

Experimental

AR-grade calcium carbonate and aluminum hydroxide gel powder were procured from Sisco Research Laboratories Pvt. Ltd. and Loba Chemie, respectively, and taken as the primary reagents in the experiments. Two types of experiments were carried out:

(1) Programmed temperature (Dynamic) runs in a Simultaneous Thermal Analyzer (STA 409 PC Luxx, Netzsch, Germany).

(2) Isothermal runs in a programmable high-temperature chamber furnace (60 F4, Okay Electric furnace, Bysakh and Co., India).

Programmed temperature experiments

The objective of these experiments was primarily to check the purity of the starting materials (so that the stoichiometric ratios of primary reagents required for C_3A phase formation can be determined) and to identify the range of temperatures in which the calcia–alumina reactions occur. Thus, simultaneous thermogravimetric (TG) analysis and differential scanning calorimetry (DSC) studies were conducted separately on calcium carbonate (up to 1000°C) and aluminum hydroxide gel powder (up to 1200°C) at a constant heating rate of 10°C min^{-1} in a N_2 atmosphere using a platinum pan. The instrument was previously calibrated using standards provided by the manufacturer. Based on the observed total mass loss of individual powders, the powders were mixed together (sieved and mixed in a cyclohexane slurry as described later) so as to give a mole ratio of $CaCO_3$:$Al(OH)_3$ equal to 3:2. About 10–15 mg of the mixture was then heated to 1200°C in the STA instrument (TG-DSC mode), keeping all other conditions fixed as in the case of the separate TG-DSC study on $CaCO_3$ and $Al(OH)_3$. The experiment was repeated in an air atmosphere to verify the effect, if any, of the gas environment on the phase formation.

Isothermal experiments

The objective of the isothermal experiments was to investigate in detail the kinetics and mechanisms of the solid–solid processes involved. In view of the disparity of results seen in the literature on various aspects of the reaction, a variety of protocols were chosen to conduct the reaction so as to establish the effect of the selected experimental variables. These protocols are typical of the procedures adopted in the literature and in industrial practice. The same mixture as above—3:2 mole ratio of calcium carbonate and aluminum hydroxide gel—was used and a high-temperature chamber furnace was used to conduct the reactions. Both powder mixtures and pellets were used in these experiments, to see the effect of particle–particle contact. In the case of powders, any effect of mechanical activation was also investigated.

Powder experiments

Two protocols were followed as described below for preparing the powder mixture for reaction, to ascertain whether mechanical activation (say resulting from ball milling) has a measurable influence on the kinetics.

- In the first protocol (*ball-milled case*), the powder samples of the two starting materials were mixed together in a planetary ball mill (Retsch, model S1, Hahn, Germany) for 25 min (grinding medium: 12 steel balls, each of 20 mm diameter) and then subjected to reaction in the programmable temperature furnace.
- In the second protocol (*slurry-mixed case*), the powder mixture for reaction was prepared as follows. Calcium carbonate and aluminum hydroxide gel powders, individually passed through a 53-μm sieve, were taken in the required ratio and slurried in cyclohexane to achieve thorough mixing. The mixture was stirred for 30 min and then dried in an oven maintained at 55°C.

Platinum crucibles were used to carry out the reactions in all cases. In the initial experiments on ball-milled powders, when the powder was introduced into the chamber furnace maintained at the reaction temperature, the rapid decomposition and dehydration reactions at the high temperature caused some spillage of the powder from the crucible. The powder was therefore introduced into the furnace at a sufficiently low temperature for these reactions to be unimportant (say 600–650°C), and the furnace temperature was then raised to the required value at 20°C min^{-1}. Reaction time was counted from the instant the furnace reached the required temperature and a zero-time sample was taken at this point. Alternatively, and in all experiments on slurry-mixed powders, the powders were heated at 800°C for 1 h in a separate furnace before being introduced into the chamber furnace maintained at the temperature of interest. Reaction time was counted from the instant of introduction of the powder into the high-temperature furnace. X-ray diffraction (XRD) studies, carried out on samples heated at 800°C for 1 h, confirmed the complete decomposition of $CaCO_3$ and the absence of any solid–solid reaction between CaO and Al_2O_3. In all cases, the samples were taken out after the required time, air-quenched, and stored in a desiccator for further analysis by quantitative XRD (QXRD, described below).

To eliminate the effect of particle size variation on XRD patterns, reacted samples in all cases were ground in an agate mortar-and-pestle and the entire amount of sample was then passed through the 53-μm sieve again, before phase quantification using QXRD. Only data from runs where all these precautions were followed and particle size of the primary reagents were the same were used for kinetic interpretation. In all cases, particle size distributions were recorded using a GALAI CIS-1 instrument (Migdal Haemek, Galil, Israel) using methanol as a suspending medium. In some cases, the

results were checked by dynamic light scattering (Brookhaven Zeta Plus) and optical microscopy.

Pellet experiments

The objective of these experiments was to study the reactions under conditions of improved particle contact. Green density measurements of powders and compacts showed that particle packing improves with pelletization pressure up to a point, beyond which it remains substantially constant. Based on these results, pellets of 12-mm diameter were prepared using an isostatically cold press at 300 MPa. These were subjected to reaction in the programmable-temperature chamber furnace. Two protocols, with different initial conditions for reaction, were followed in these experiments:

- In the first (*pretreated pellets*), green pellets of 3:2 mole ratio calcium carbonate and aluminum hydroxide gel powder were heated to 800°C in a furnace and maintained at that temperature for 1 h to complete the formation of the oxides from the starting materials, before introducing them into the high-temperature chamber furnace maintained at the temperature of interest. As in the case of the powder experiments, XRD analysis confirmed the complete decomposition of $CaCO_3$ and the absence of any solid–solid reaction between CaO and Al_2O_3 as a result of the pretreatment.
- In the second (*raw pellets*), green pellets of the same powder mixture were directly introduced into the chamber furnace at the reaction temperature and reacted for the required length of time.

In both cases, all the necessary precautions listed above were taken. A platinum crucible was used and reactions were carried out for different times. After the required length of time, pellets were removed from the furnace, air-quenched, and stored for the QXRD analysis.

Quantitative X-ray diffraction (QXRD)

Phase quantification was done using QXRD by the Internal Standard Method[26] using TiO_2 (rutile) as internal standard. A fixed amount (14.65%) of the internal standard, which was also passed through the 53-μm sieve, was added to each ground sample and the entire composite mixed together under cyclohexane. The mixture was then dried and examined by Philips X'Pert PRO diffractometer using Cu as a target at a voltage of 40 kV and current of 30 mA. Randomly oriented samples were prepared by a back-loading technique to avoid preferential orientation. Scans were taken for a 2θ range of 5–75° with a step size of 0.017°.

For any given phase, the intensity ratio of one of the nonoverlapping peaks (the reference peak, preferably the most intense) of that phase with one of the nonoverlapping peaks of rutile was calculated from the diffractogram, and the mass percentage of the phase present was calculated using this intensity ratio and the calibration constant (described below). The relative intensities and reference peaks used in the quantification are listed in Table 3. To prepare calibration curves for each of the phases of interest (C_3A, $C_{12}A_7$, CA, CA_2), the pure phases were synthesized by repeated heating and grinding of the oxides taken in the necessary stoichiometric proportion, until there was no trace of the starting oxides. XRD patterns were obtained for known mixtures of these pure phases with the internal standard in the usual manner and plots of composition vs. intensity ratio (with respect to rutile) were made, from which the calibration constant (K_{cal}) for each phase was calculated using

$$\frac{I_P}{I_{is}}\frac{I_{is}^{RI}}{I_P^{RI}} = K_{cal}\frac{W_P}{W_{is}} \tag{1}$$

where I and I^{RI} are the intensity and relative intensity (with respect to the most intense nonoverlapping peak), respectively, and W is the weight of the phase in the calibration sample.

Table 3. Reference Peaks and Their Relative Intensities Used for Phase Quantification by XRD

Phase	*d*-space (Å)	Angle (2θ)	Relative Intensity	JCPDS Number
α-Al_2O_3	2.086	43.34	100	43–1484
CaO	2.405	37.347	100	37–1497
Rutile	3.248	27.436	100	78–2485
C_3A	1.557	59.272	24.0	38–1429
$C_{12}A_7$	4.891	18.122	100	78–0910
CA	2.966	30.13	100	23–1036
CA_2	4.440	19.997	55.0	23–1037

Results and Discussion

The raw powders (as received) had the following size characteristics: $CaCO_3$:0.5–12.0 μm (mean size about 1.9 μm); $Al(OH)_3$:0.5–4.0 μm (mean size about 1.05 μm). In all powder experiments except those with ball-milled powders, the particle size of the mixture were in the range 0.5–6 μm with an average particle size of about 1.7 μm. In the case of the ball-milled powder mixture, the particles were in the size range 0.5–2 μm with a mean size of 1.0 μm. Some size reduction thus occurs during ball-milling, apart from mixing. However, it is of interest to see whether the particle reactivity is affected.

Programmed temperature (TG-DSC) experiments

The results of the TG-DSC study on calcium carbonate showed an endothermic DSC peak at 794.1°C with extrapolated onset temperature 725.4°C, corresponding to its decomposition.[27] The mass loss shown by TG is 43.77%, which agrees well with the expected value of 44.0% for complete removal of CO_2. The ΔH shown by DSC of 1794 J g^{-1} compares with 1794 J g^{-1} for $CaCO_3$ decomposition.[28] In the case of aluminum hydroxide gel powder, two broad endothermic DSC peaks were observed at 99.5 and 278.1°C corresponding to adsorbed (unbound) moisture loss and dehydration, respectively. The peaks are not well resolved under these conditions. The total mass loss was found to be 42.47%, most of which (39.90%) occurs in these two stages at $\leq$600°C. In addition, two exothermic DSC peaks were observed at 848.8 and 1107.8°C, with no corresponding DTG peaks. These are attributed to the phase transformation of Al_2O_3 formed after dehydration of $Al(OH)_3$.[29] The observations indicate that conversion to the oxide is complete by 600°C. Therefore, 600–650°C was chosen as the temperature of introduction of the powder samples into the chamber furnace, as described previously.

Based on the above results, a mixture of $CaCO_3$ and $Al(OH)_3$ so as to give a 3:1 mole ratio of CaO:Al_2O_3 was made and a TG-DSC study conducted. The results are shown

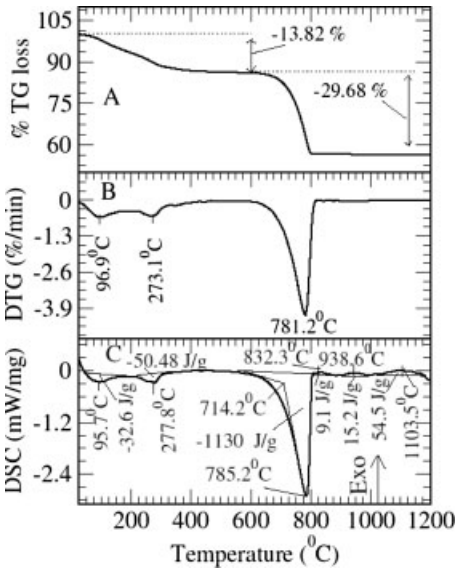

Figure 1. Thermal analysis results on $CaCO_3$ and $Al(OH)_3$ gel mixture (3:2 mole ratio).

(A) TG curve, (B) DTG curve, and (C) DSC curve.

in Figure 1. A total weight loss of 43.50% was observed in two stages (13.82 + 29.68% in Figure 1A) corresponding to adsorbed moisture loss and dehydration of $Al(OH)_3$ up to 600°C and calcination of $CaCO_3 > 600$°C, respectively (such a two-stage decomposition was also observed by Rivas Mercury et al.[2]). The corresponding DTG peaks are shown in Figure 1B. This total mass loss matches well with the mass loss of 43.42%, calculated from the individual mass losses observed with pure $CaCO_3$ and $Al(OH)_3$ gel. The first stage up to 600°C contributes 13.82% [calculated value 14.81% arising mainly from dehydration of $Al(OH)_3$] and the second stage contributes 29.68% (calculated value 28.60%, arising from decomposition of $CaCO_3$). These stages correspond to the three endothermic DSC peaks at 95.7, 277.8, and 785.2°C in the DSC curve of Figure 1C. A downward shift of all these peaks from their positions in pure samples was observed and is noteworthy. A downward peak shift is also observed for the exothermic peaks of alumina phase transition (832.3 vs. 848.8°C and 1103.5 vs. 1107.8°C). An additional broad exothermic DSC peak was observed at 938.6°C, indicating the formation of calcium aluminate phases resulting from solid–solid reactions between Al_2O_3 and CaO; this corresponds to no weight loss in TG curve of Figure 1A. TG-DSC experiments in an air atmosphere gave exactly identical results to the above, showing no influence of the gas environment.

The following reactions lead to the oxides from the starting materials:

- Dehydration of aluminum hydroxide[2]

$$.2Al(OH)_3\ (s) \rightarrow Al_2O_3\ (s) + 3H_2O\uparrow(g) \qquad (2)$$

- Decarboxylation of calcium carbonate

$$.CaCO_3\ (s) \rightarrow CaO\ (s) + CO_2\uparrow(g) \qquad (3)$$

The reactions possible among these oxides and the primary reaction products are described in a later section.

Isothermal experiments in the chamber furnace

Powder Experiments. Experiments with powder mixtures were performed in the temperature range of 1100–1300°C and the variation of mass fractions of different phases observed with time have been plotted for different temperatures, for ball-milled and slurry-mixed powder samples, in Figures 2 and 3, respectively. It is clear that there are significant differences in kinetics between the two cases. Further, the following observations may be made:

- The conversion of alumina (as given by the sum of the product phases) is in general quite fast. In fact, in the case of ball-milled samples at the higher temperatures, a significant amount of conversion takes place even before the desired reaction temperature is reached, as seen by the conversion in the zero-time samples (Figure 2).
- In all, three calcium aluminate phases are seen: CA, $C_{12}A_7$, and C_3A as observed by Williamson and Glasser[5] and Mohamed and Sharp.[14] The mass fraction of C_3A increases continuously as is expected of a final product. The other two phases, where observed, show characteristics of intermediates, their amounts increasing initially and decreasing at long times. At the higher temperatures with ball-milled powders, the data capture only the declining phase because the maximum is probably already past by the time the mixture reaches the reaction temperature.
- The CA phase was observed only in ball-milled samples. This may be attributable either (1) to local inhomogeneities in these samples, leading to local compositions different from the average composition taken, or (2) to mechanochemical activity itself, the formation and consumption reactions of CA being promoted to different extents. Similar results were previously reported by Rivas Mercury et al.[2] when they attempted to produce C_3A from mechanochemically activated precursors such as $CaCO_3$ and $Al(OH)_3$.

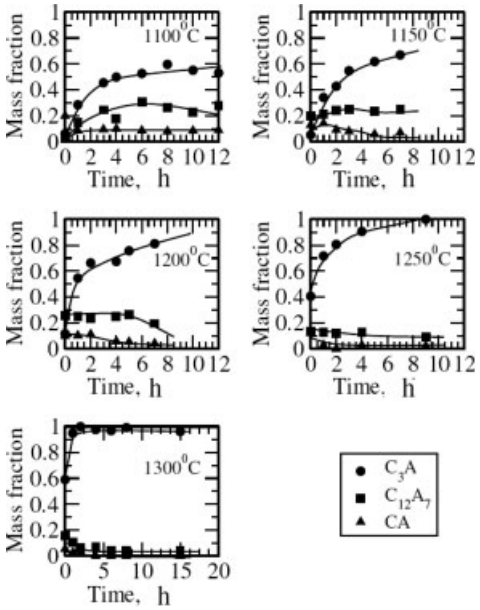

Figure 2. Variation of product phase mass fractions with time at different temperatures for ball-milled powder mixtures.

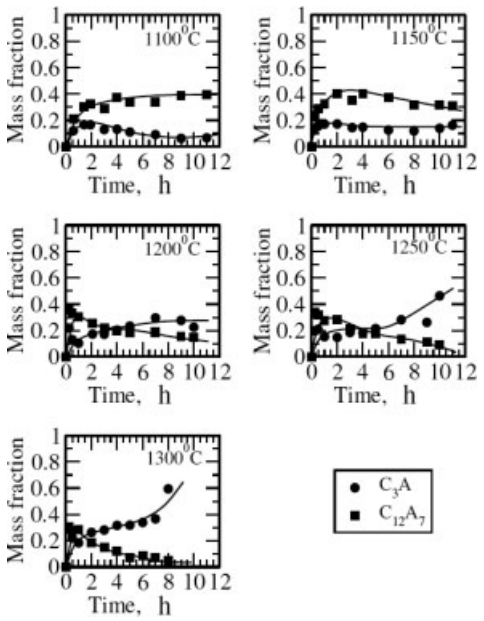

Figure 3. Variation of product phase mass fractions with time at different temperatures for slurry-mixed powder mixtures.

- No other phases like CA_6 and CA_2 were observed in any of the experiments as observed by others.[2,14] Lower temperatures may be needed to make these phases with excess alumina in the reaction mixtures.
- Where the CA phase is seen (ball-milled powders), it is present in much smaller amounts and peaks earlier than $C_{12}A_7$, indicating that it is more reactive (because of its metastable nature at the prevailing condition[30]) and is a precursor to $C_{12}A_7$ in the reaction sequence. At 1300°C, the amount of CA phase was reduced to zero just after the first hour.
- In both cases (Figures 2 and 3), the amount of C_3A phase at any time was found to increase with temperature; at a particular temperature it generally increases with the heating time. At low temperatures, the C_3A mass fraction nearly levels off after a certain time, with significant amounts of the other phases still remaining, whereas at higher temperatures, the mass fractions of all phases except C_3A go to zero. This suggests an incomplete conversion of the intermediates to the final product at low temperatures. Similar incomplete conversion of a reactant has been observed in gas–solid reactions,[31] where it has been attributed to pore closure.
- In both cases, the rate of decrease of $C_{12}A_7$ is the more pronounced, and its maximum mass fraction the lower, the higher the temperature.
- In ball-milled samples, the amount of phases found follow the sequence $C_3A > C_{12}A_7 > CA$ from very small times. Although the trend is not as clear in the slurry-mixed case, it is generally seen that the mass fraction of C_3A increases as that of $C_{12}A_7$ decreases. These features indicate the "reaction intermediate" status of $C_{12}A_7$ and show that the conversion of intermediates to the final product is much faster in the ball-milled case.

Interestingly, in many experiments with slurry-mixed powders, the initial C_3A formed seems to decrease before increasing again, as expected of a final product in the reaction sequence. This is as though C_3A first formed becomes converted by a reverse reaction with alumina to an "intermediate" phase before the invading calcia converts it back. This trend has not been reported previously and reasons are not clearly understood. It is possible that the explanation has to do with changes in the porous structure, and consequently diffusivity, as the particles are progressively converted. Local inhomogeneities and poor particle contact could also have played a role because, as will be seen further, these peculiarities were not observed in the pellet experiments. Thus the possibility that it is an artifact in the powder experiments cannot also be ruled out.

It is clear from the above observations that ball milling profoundly influences the subsequent kinetics of calcia–alumina reaction. This is suggestive of significant mechanical activation of the reactant during ball milling. Figure 4 shows the XRD pattern of $CaCO_3$ powder before and after the ball milling under the conditions followed in the experiments. The degradation in the pattern is again evidence of mechanochemical activation.[27] The activation in the present case is such that there is considerable reaction even before the reaction temperature is reached in the case of ball-milled powders, something not expected from the rates seen in the other case. The reaction thus seems to begin at lower temperatures arising from activation. Further, rates of conversion at equal conversions are clearly higher. $C_{12}A_7$ conversion kinetics also seems faster in the ball-milled samples, as seen by the lower size of peaks and faster disappearance rates in the latter case. If $C_{12}A_7$ is regarded as an intermediate that further converts to C_3A, the above two trends are consistent.

The above observations are significant because mixing in ball mills is common practice in industrial and scientific studies on such reactions.[32,33] The literature also contains references to mechanochemical activation when powders are mixed in a ball mill.[2,27,34,35] The proliferation of crystal defects during ball milling is said to be responsible for the activation.[2] In fact, this forms the basis of an alternative route to synthesize calcium aluminates.[34]

Pellet Experiments. The kinetics of C_3A formation in pelletized calcia–alumina systems was studied for both *pretreated pellets* and *raw pellets*, in the temperature range of

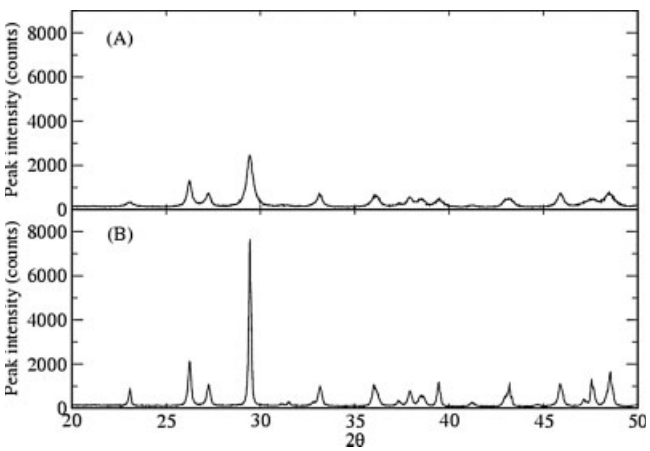

Figure 4. XRD of $CaCO_3$ powder.

(A) After ball milling; (B) before ball milling.

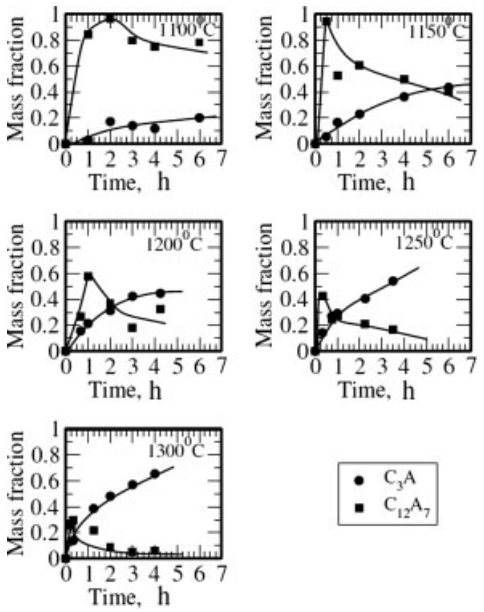

Figure 5. Variation of product phase mass fractions at different temperatures in the case of pretreated pellets.

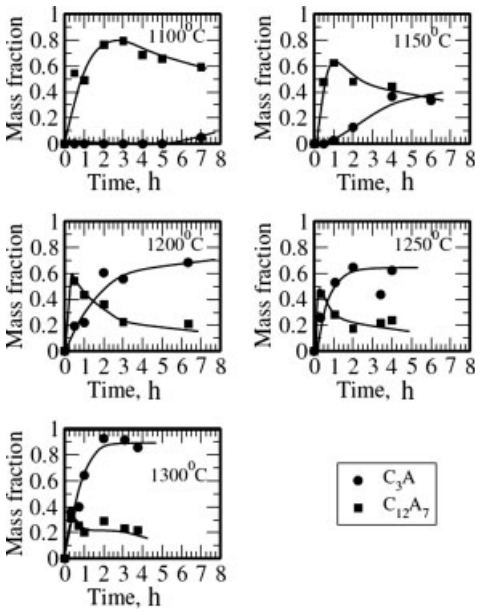

Figure 6. Variation of product phase mass fractions at different temperatures in the case of raw pellets.

1100 to 1300°C. The only calcium aluminate phases observed in these experiments were $C_{12}A_7$ and C_3A. Figures 5 and 6 show the variation of mass fractions of these phases with time at the temperatures studied, for the two cases. The mass fraction of $C_{12}A_7$ was found to increase initially and then gradually decrease with a simultaneous increase of C_3A phase. This trend, even more conclusive here (under conditions of better interparticle contact) than in the case of powders, indicates that $C_{12}A_7$ is the intermediate to C_3A formation. The difference here is that, presumably because of the improved contact between the reactant particles, the CA phase is not observed at all.

A comparison of the rates of phase formation for two cases each of powder and pellet experiments shows some interesting features (Figure 7). The following are noteworthy:

- The ball-milled samples show the highest rates of C_3A formation. At the lower temperatures, only these samples show sufficiently high rates to reach high conversions within the experimental time. Thus for example at 1100°C, C_3A levels reached almost 53% in 6 h of reaction in these samples, in contrast to only $\leq$20% in slurry-mixed powders and pretreated pellets, and 0% in raw pellets. The importance of mechanical activation in ball-milled samples is thus revealed; the activation is such as to override the negative effect of poor particle contact in the powders.
- Among the non-ball-milled samples, the pellet experiments show a higher rate of reaction than that of the powder experiments, indicating that particle–particle contact plays an important role in determining the kinetics of phase formation by solid–solid reactions.
- The rates of C_3A formation are usually in the order: ball-milled powder $\geq$ raw pellets $\geq$ pretreated pellets $\geq$ slurry-mixed powder (except at 1100°C). In the case of pretreated pellets, the decomposition reactions of the primary reagents occur in a smooth and controlled manner as the temperature is gradually raised to the reaction temperatures observed in TG-DSC studies. The evolution of the decomposition products and creation of porosity also proceed smoothly and there is a high likelihood of the final physical structure being the same in every experiment. In the case of raw pellets, which are suddenly exposed to the reaction temperatures, these reactions are likely to occur violently. Some extent of defect generation in a manner akin to mechano-

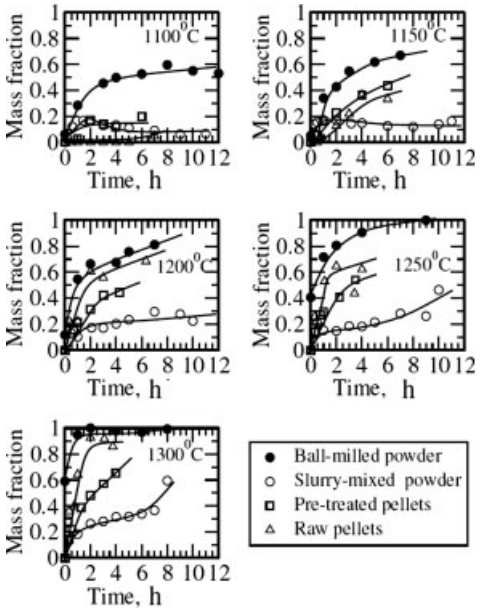

Figure 7. Comparison of C_3A phase formation rates at different temperatures in powder and pellet experiments.

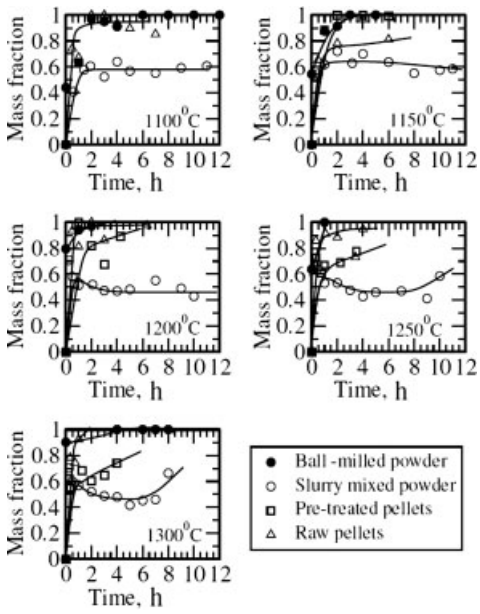

Figure 8. Comparison of alumina conversion rates at different temperatures in powder and pellet experiments.

chemical activation is thus possible in this case. Further, the violent release of the decomposition products introduces a random element to the final porous structure that is then presented to the solid–solid reactions, and this could have an effect on the rates of transport phenomena in this case. The greater scatter of the data in the case of raw pellets is indicative of such a phenomenon.

• Although the raw pellets show no C_3A up to 6 h of reactions at 1100°C, Figure 6 shows considerable conversion of alumina to $C_{12}A_7$. This indicates that formation of $C_{12}A_7$ is a fast step and conversion of the already-formed $C_{12}A_7$ to C_3A is the slowest step. To see this more clearly, conversions of alumina (calculated from the totality of products) in all four cases are shown in Figure 8. The initial rates of disappearance of alumina (when alumina particles are more exposed) are seen to be very fast in all the cases.

Reaction intermediates and reaction sequence

Many reactions are possible among the oxides, leading to various calcium aluminate phases, such as C_3A, $C_{12}A_7$, CA, CA_2, and CA_6. These can further react among themselves or with the oxides. For example, some of the suggested reactions are[13]

$$CA\ (s) + 2CaO\ (s) \rightarrow C_3A\ (s) \quad (4)$$

$$CA_2\ (s) + 5CaO\ (s) \rightarrow 2C_3A\ (s) \quad (5)$$

$$C_{12}A_7\ (s) + 9CaO\ (s) \rightarrow 7C_3A\ (s) \quad (6)$$

$$C_{12}A_7\ (s) + CA\ (s) + 11CaO\ (s) \rightarrow 8C_3A\ (s) \quad (7)$$

Evidence on the sequence of intermediate and minor phase formation in the literature is confusing. Although Gulgun et al.[36] conclude that the sequence of phase formation is always from calcium-rich phases to the phase for which reaction mixture is proportioned, experimental findings of Mohamed and Sharp[14] and Kohatsu and Brindley[7] indicate the reverse sequence, that is, a sequence that proceeds from alumina-rich phases toward the phase for which the reaction mixture is proportioned. Experimental studies on the subject fall into two main groups. In the first, reaction couples consisting of sintered pellets of CaO and Al_2O_3 are fired. Several or even all of the five calcium aluminate phases have been observed in these studies. As the reacted pellet is scanned from the lime end to the alumina end, the phases are seen as parallel zones, with the concentration of calcium gradually decreasing and that of aluminum increasing.[7] The general agreement seems to be in favor of Ca^{2+} diffusing through the reaction product toward the alumina pellet.[37] The "marker experiments" of Weisweiler and Ahmed[9] on the calcium aluminate system using Pt as marker may also be cited in the same context. In the second group, powder mixtures of CaO and Al_2O_3 are fired and different observations have been reported. Williamson and Glasser[5] reported $C_{12}A_7$ to be the principal nonequilibrium phase, although CA was also observed. Mackenzie and Banerjee[8] identified C_2A, $C_{12}A_7$, CA, CA_2, and CA_6 during the synthesis of C_3A, but concluded that CA_2 and C_2A were reaction intermediates, whereas the remaining phases were considered as minor products. Singh et al.[13] also reported several calcium aluminate phases when a 3:1 mixture of CaO and Al_2O_3 was fired at 1380°C. Chou and Burnet[11] suggested that $C_{12}A_7$ is likely to be the first compound formed, but the amount present initially does not grow to any appreciable extent. CA is then formed as the CaO continues to diffuse into the Al_2O_3. After the alumina particle is completely converted into CA, the C_3A phase begins to form. After both Al_2O_3 and CaO are expended, $C_{12}A_7$ grows at the expense of CA and C_3A. Mohamed and Sharp[14] reported $C_{12}A_7$ and CA as the intermediates of C_3A formation.

Williamson and Glasser[5] refer to the thermodynamic studies on the CaO–Al_2O_3 system by Mchedlov-Petrosyan and Babushkin,[38] which show that $C_{12}A_7$ is the first calcium aluminate phase formed <1000°C and at >1100°C it ceases to be an important metastable phase. It is also shown that the C_3A phase does not form directly from CaO and Al_2O_3 but only by the reaction of $C_{12}A_7$ with CaO. Previous programmed temperature (TG-DSC) study and isothermal experimental results also support the conclusion that $C_{12}A_7$ is the only intermediate in C_3A formation if powders are well mixed before reaction and the particles are in good contact.

In our experiments, the CA phase was found only when ball-milled powder mixtures were reacted, and not in slurry-mixed or pelleted mixtures. A comparison of all our results suggests that conclusions on reaction kinetics and the sequence of phase formation are better based on experiments carried out under conditions of good particle contact and in which the reacting entity is formed in a manner that ensures a reproducible physical structure. Our results from such experiments favor a sequence of phase formation that starts with alumina-rich phases and moves toward C_3A, which in our case is the equilibrium phase for which the reaction mixture is proportioned.

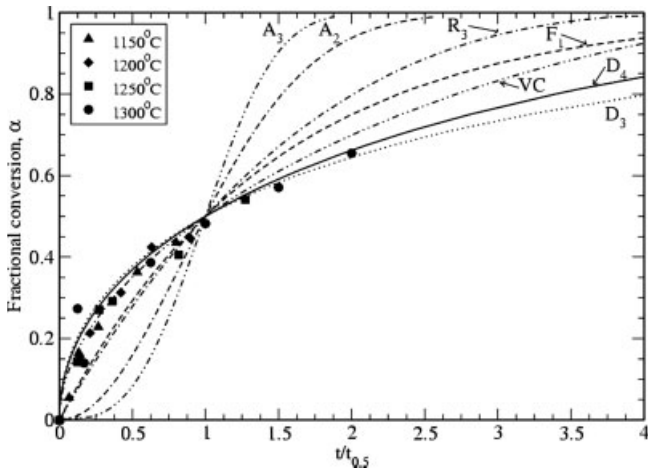

Figure 9. Reduced time plot α vs. $t/t_{0.5}$, assuming fraction of Al_2O_3 converted (α) = fraction of Al_2O_3 in C_3A (pretreated pellets).

Kinetics of calcia–alumina reactions

In view of the demonstrated importance of interparticle contact, in this work kinetics were determined only from pellet experiments. In the literature on calcium aluminate kinetics, the mass fraction of the product C_3A has commonly been used in place of conversion (α in the expressions of Table 1), both in model selection and in parameter evaluation. For the purpose of comparison, in this work also the same practice is adopted to start with. The applicable kinetic models were determined using the method of reduced time plots.

Because model discrimination involves making plots of C_3A mass fraction against reduced time ($t/t_{0.5}$), temperatures at which the highest mass fractions realized were <0.5 were excluded. From data at the other temperatures, $t_{0.5}$ for normalization is determined for each temperature as the time at which C_3A mass fraction reaches 0.5. Data are compared with different models (Table 1) in the reduced-time plots of Figures 9 and 10, respectively, for pretreated and raw pellets.

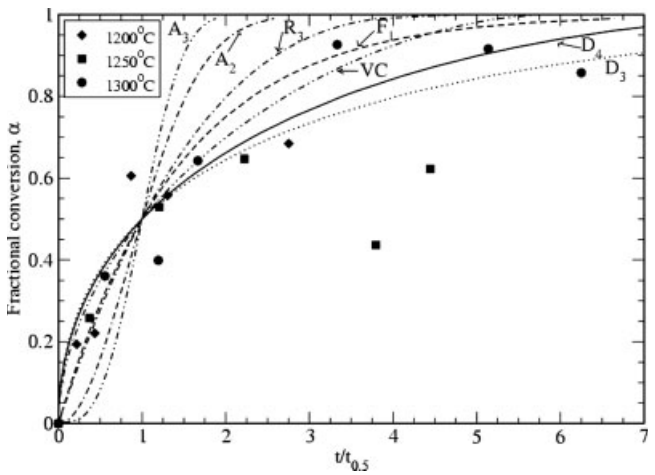

Figure 10. Reduced time plot α vs. $t/t_{0.5}$, assuming fraction of Al_2O_3 converted (α) = fraction of Al_2O_3 in C_3A (raw pellets).

Table 4. Physical Parameters from Literature for Different Calcium Aluminate Phases

	Different Phases			
Physical Parameter	C_3A	$C_{12}A_7$	CA	Al_2O_3
Density (kg m^{-3})[10]	3030	2700	2980	3990
Oxygen packing density (kg m^{-3})[13]	1170	1030	1210	1870
z (for VC model)[10]	3.49	2.87	2.08	—

D_1, being a one-dimensional diffusion model, was omitted from consideration. Among the other models, the Valensi–Carter model is the only one that accounts (in some manner) for a change in volume resulting from the reaction. The densities of the relevant solid phases, given in Table 4, indicate that volume change could indeed be important.

It is seen that the scatter of data in the case of raw pellets is more than that in the data from pretreated pellets, and possible reasons have been elaborated on earlier. From the figures (Figures 9 and 10), D_3 (Jander) and D_4 (Ginstiling–Brounshtein) models would seem to best fit the data, although the fit of the VC (Valensi–Carter) model is also reasonable. Accordingly, plots of the functions $D_4(\alpha)$, $VC(\alpha)$, and $D_3(\alpha)$ vs. time have been made (Figures 11A, 11B, and 11C, respectively, for precalcined pellets and Figures 12A, 12B, and 12C, respectively, for raw pellets) and used for calculating the kinetic parameter in the models. Slopes of these lines (k) at different temperatures have been used in an Arrhenius-type plot [ln(k) vs. $10^4/T$, shown in Figures 11D and 12D] to determine the activation energy (E) and preexponential factor (A) for the three models, shown in Table 5. It is to be noted that all three models assume diffusion control, and thus the kinetic parameter referred to above is related to a diffusivity.

The activation energies reported in the literature for the calcia–alumina system, shown in Table 6, are in the range 150 to 285 kJ mol^{-1}. A comparison with the values obtained

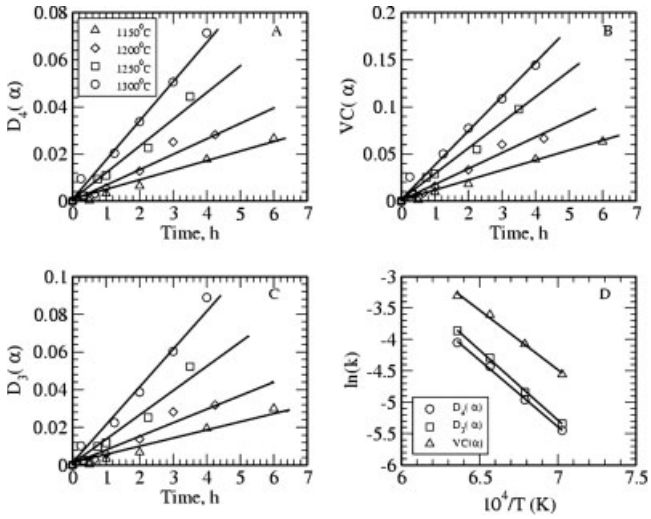

Figure 11. (A) D_4 (α) vs. t plot for Ginstling–Brounshtein model; (B) VC(α) vs. t plot for Valensi–Carter model; (C) D_3 (α) vs. t plot for Jander model; (D) ln(k) vs. $10^4/T$ plot (pretreated pellets).

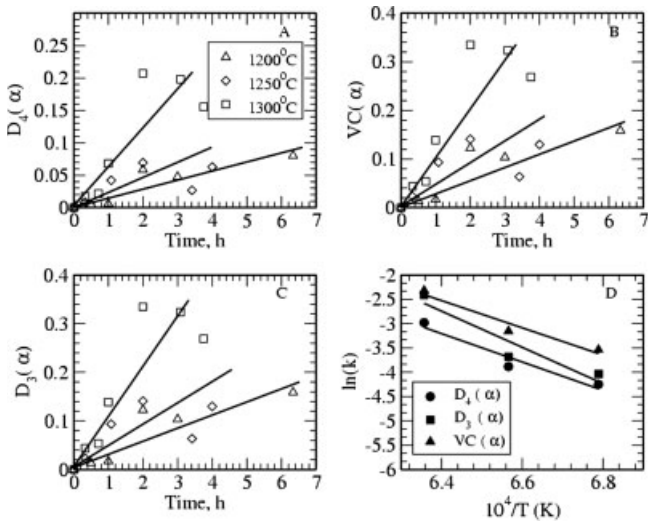

Figure 12. (A) D_4 (α) vs. *t* plot for Ginstling–Brounshtein model; (B) VC(α) vs. *t* plot for Valensi–Carter model; (C) D_3 (α) vs. *t* plot for Jander model; (D) ln(k) vs. $10^4/T$ plot (raw pellets).

in this work shows that our values for precalcined pellets agree with the lower part of this range, whereas the values for raw pellets are toward the higher end of the same range. Taken together with the analysis presented in the preceding paragraphs, these results therefore provide an explanation for the wide variation in the literature on the subject. It is worth noting that, in both cases, the values of activation energy according to the VC model are the lowest. In view of the point made earlier about phase densities, if the present modeling framework is to be followed at all, the values from the VC model are probably to be trusted more than those from the others.

It is also interesting that, for the raw pellets, not only are the rates of C_3A formation higher, but so also are the activation energies—a fact already obvious from the increasing discrepancy of the rates (as compared to the precalcined pellets) as temperature increases. We must note that several types of reaction—calcination, dehydration, and solid–solid reactions—are taking place simultaneously in the case of the raw pellets. As pointed out earlier, at the reaction temperatures, the first two of these would be extremely fast and would lead to a violent release of the gaseous decomposition products in the case of the raw pellet experiments. This could even fracture the primary particles and thus appreciably affect their reactivity; a more facile diffusion of any diffusing reactant for the solid–solid reaction would also be a possibility. The larger scatter of the data for the case of raw pellets would also be attributable to such violent events because the structure that evolves as a result would not be reproduced exactly in every experiment.

The values of activation energy (in the literature and in this work) are similar to the activation energy reported for Ca^{2+} diffusion into CaO (142–268 kJ mol^{-1}),[10] while being much less than that reported for the diffusion of Al^{3+} into Al_2O_3 (478 kJ mol^{-1}).[10] Such considerations have usually been used in the literature to suggest a mechanism that involves the diffusion of Ca^{2+} in preference to that of Al^{3+}.

Table 5. Activation Energy and Preexponential Factor for C_3A Formation in Pretreated Pellet Experiments and Raw Pellet Experiments

Pellet Experiments	Model Used	Temperature Range (°C)	*E* (kJ mol^{-1})	*A* (h^{-1})
Pretreated	D_4	1150–1300	176	1.24×10^4
	VC		157	6.44×10^3
	D_3		185	3.03×10^4
Raw pellets	D_4	1200–1300	243	5.41×10^6
	VC		233	5.06×10^6
	D_3		310	1.48×10^9

There is also support in the literature of a different kind for such a hypothesis, in the form of marker experiments (see, for example, the studies of Weisweiler and Ahmed[9] on calcium aluminate system using Pt as marker). In our opinion, it is safer to rely on such direct evidence rather than infer the mechanism from the values of parameters such as activation energy because, as will be discussed further, the models used (of which the activation energy becomes a parameter) need to be considered more carefully than has normally been done in the literature.

Comments on the Suitability of 'Single-reaction' Models

The results of this work in terms of the multistep nature of the reaction and the "intermediate" status of phases such as $C_{12}A_7$ in the reaction network, taken together with suggestions in the literature based on direct evidence, are strongly suggestive of a mechanism that involves the fast conversion of alumina, by diffusing Ca^{2+}, to intermediate(s) ($C_{12}A_7$ being the prominent one), which is (are) then slowly converted to the final product C_3A, again by the diffusing calcium. Other supporting evidence such as the oxygen packing density of the calcium aluminate phases (see Table 4) can also be cited in favor of such a hypothesis. Thus the following scheme can be taken as a plausible mechanism for the formation of tricalcium aluminate:

$$3CaCO_3 + 2Al(OH)_3 \xrightarrow{-H_2O,-CO_2} 3CaO + Al_2O_3 \longrightarrow C_{12}A_7 \xrightarrow{CaO} C_3A \quad (8)$$

The models used above for data interpretation are all derived for a single reaction, not a sequential reaction scheme suggested by the data.

In view of the above, the reasonable agreement the single-reaction models provide to the data is intriguing. The matter has to be seen in the proper perspective, however. The usual practice of using the mass fraction of C_3A in place of frac-

Table 6. Activation Energy Values for C_3A Formation from the Literature

Reagent	*E* (kJ mol^{-1})	Model
$CA_2/CaCO_3$	[6]285	—
$CaCO_3/Al_2O_3$	[8]203	D_4
$CaCO_3/Al_2O_3$	[9]151	D_1
$CaCO_3/Al_2O_3$	[11]191	D_4, VC
$CaCO_3/Al_2O_3$	[14]216 ± 10	D_4
$CaCO_3/Al(OH)_3$	[14]224 ± 10	D_4

tional conversion of alumina (α), as done above (and in the literature), is justifiable only when C_3A is the only product. When appreciable amounts of other "product" phases are present, the alumina converted has to be calculated by considering the totality of all products. Conversion thus calculated is shown plotted on the master plot (showing the different models) in Figures 13 and 14 for precalcined and raw pellets, respectively. Note that $t_{0.5}$ values for these plots are also based on total conversion profiles as shown in Figure 8. Because of the rapid conversion of alumina, as pointed out earlier, there is much greater uncertainty on the values of $t_{0.5}$ in this case. Even accounting for this, one no longer sees the kind of agreement with the models seen earlier. The inadequacy of the single-step models in describing the complex kinetics of calcia–alumina reaction is thus exposed. Models that take into account the nature of the reaction network within the shrinking core framework are being developed and tested and will constitute the subject of a further article on the subject.

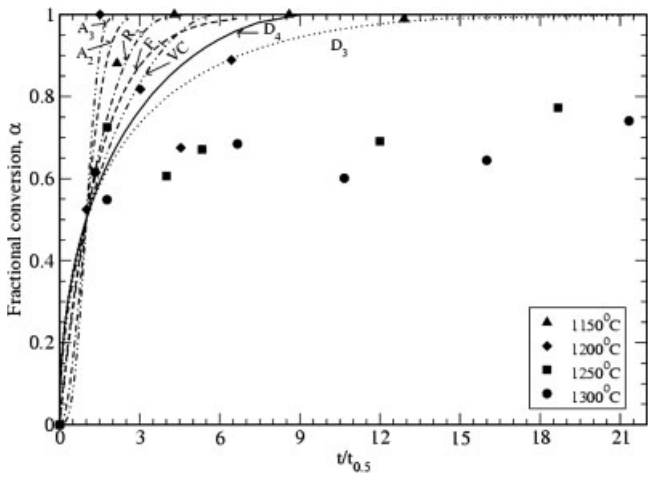

Figure 13. Reduced time plot of α vs. $t/t_{0.5}$ for pretreated pellets, where α is fraction Al_2O_3 reacted.

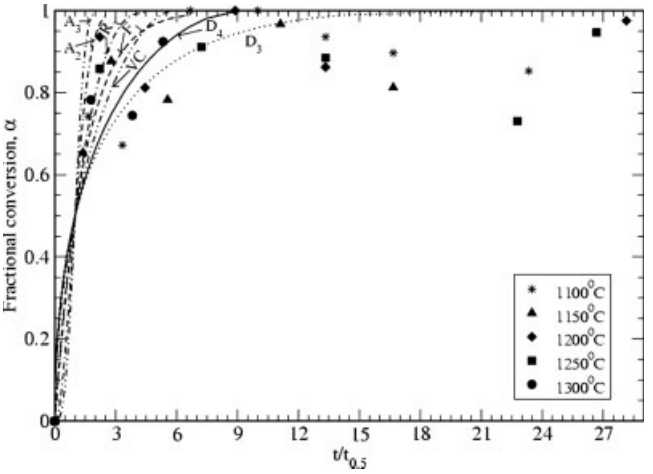

Figure 14. Reduced time plot of α vs. $t/t_{0.5}$ for raw pellets, where α is fraction Al_2O_3 reacted.

Conclusions

Reactions between calcium oxide and aluminum trioxide, starting with $CaCO_3$ and $Al(OH)_3$ gel as raw materials as in the cement industry, have been studied in the temperature range 1100–1300°C in this work. To explain the disagreements between different authors in the literature, a variety of conditions were used to clarify the significance or otherwise of experimental variables such as the method of mixing, interparticle contact, and the effect of precalcination and dehydration before solid–solid reaction. The results provide a clear incidence of mechanochemical activation when the powders are mixed in a ball mill, as opposed to a procedure in which a liquid slurry is followed by solvent evaporation. Mechanochemical activation could have significant implications for industrial practice; thus obtaining consistent and reproducible results for these cases forms the subject of an ongoing study in our laboratory. Particle size, size distribution, and good interparticle contact are additional important variables. Clearly, all of these have to be tightly controlled to achieve reproducible and reliable kinetic measurements. Reproducible and consistent kinetic data can be obtained under conditions of good physical contact between particles and by ensuring that the physical structure of the entity that finally reacts in a solid–solid reaction is created in a reproducible manner. In passing, it may be observed that the importance of physical structure shows the possible significant role of transport steps in the reaction.

Our results also unambiguously establish the multistep nature of the reaction to form tricalcium aluminate. Although a number of intermediate phases are possible, under conditions of good interparticle contact and high temperatures, $C_{12}A_7$ is the sole intermediate. The kinetics, when interpreted in the traditional manner, do show consistency with some of the diffusion-control models often used in this context. However, when intermediate phases are properly accounted for in reckoning reactant conversion, the models are seen to be inadequate. The need for a model that explicitly accounts for the multistep nature of the reaction is thus highlighted. Our ongoing work addresses some of these issues.

Notation

A = preexponential factor, h^{-1}
E = activation energy, kJ mol^{-1}
I = Intensity of peak, counts
K = constant
k = rate parameter, h^{-1}
R = gas constant, J mol^{-1} K^{-1}
t = time, h
T = temperature, K
W = weight, g
z = volume of product formed from unit volume of reactant

Greek letters

α = fractional conversion
θ = angle in degree

Subscripts

cal = calibration
is = internal standard
P = any phase

Superscript

RI = relative intensity

Literature Cited

1. Taylor HFW. Cement Chemistry. London: Academic Press; 1964.
2. Rivas Mercury JM, De Aza AH, Turrillas X, Pena P. The synthesis mechanism of $Ca_3Al_2O_6$ from soft mechanochemically activated precursors studied by time resolved neutron diffraction up to 1000°C. *J Solid State Chem*. 2004;177:866–874.
3. Yang S, Kondo JN, Hayashi K, Hirano M, Domen K, Hosono H. Partial oxidation of methane to syngas over promoted $C_{12}A_7$. *Appl Catal A: Gen*. 2004;277:239–246.
4. Oh SH, Finones R, Choi SY, Kim KN. Influence of tricalcium aluminate phase on in vitro biocompatibility of calcium aluminate bone cement. *J Mater Res*. 2004;19:1062–1067.
5. Williamson J, Glasser FP. Reactions in heated lime-alumina mixtures. *J Appl Chem*. 1962;12:535–538.
6. Repenko KN. Synthesis of calcium aluminates. *Sb Nauchn Tr Ukr Nauchn-Issled Inst Ogneuporov*. 1963;7:318–329.
7. Kohatsu I, Brindley GW. Solid state reactions between calcium oxide and α-aluminium oxide. *Z Phys Chem*. 1968;60:79–89.
8. Mackenzie KJD, Banerjee RK. Formation kinetics of Portland Cement clinker phases: I—Tricalcium aluminate. *Trans J Br CERM Soc*. 1978;77:88–92.
9. Weisweiler W, Ahmed SJ. Kinetics of solid state reactions in the system calcium aluminium oxide. *Zement-Kalk-Gips*. 1980;33:84–89.
10. Singh VK, Ali MM. Formation kinetics of high alumina cement phases: I—Monocalcium aluminate. *Trans J Br CERM Soc*. 1980;79:112–114.
11. Chou KS, Burnet G. Formation of calcium aluminates in the lime-sinter process, Part II: Kinetic study. *Cement Concrete Res*. 1981;11:167–174.
12. Singh VK, Mondal UK. Kinetic study of the thermal synthesis of calcium dialuminate above 14000C. *Trans J Br CERM Soc*. 1982;81:112–113.
13. Singh VK, Ali MM, Mandal UK. Formation kinetics of calcium aluminates. *J Am CERM Soc*. 1990;73:872–876.
14. Mohamed BM, Sharp JH. Kinetics and mechanism of formation of tricalcium aluminate, $Ca_3Al_2O_6$. *Thermochim Acta*. 2002;338:105–114.
15. Sharp JH, Brindley GW, Achar BNN. Numerical data for some commonly used solid state reaction equations. *J Am CERM Soc*. 1966;49:379–382.
16. Tamhankar SS, Doraiswamy LK. Analysis of solid–solid reactions: A review. *AIChE J*. 1979;25:561–582.
17. Scian AN, Porto López JM, Pereira E. High alumina cements. Study of $CaO{\cdot}Al_2O_3$ formation. II: Kinetics. *Cement Concrete Res*. 1987;17:525–531.
18. Ali MM, Raina SJ, Singh VK. Kinetics and diffusion studies in CA_2 formation. *Cement Concrete Res*. 1989;19:47–52.
19. Mohamed BM, Sharp JH. Kinetics and mechanism of formation of monocalcium aluminate, $CaAl_2O_4$. *J Mater Chem*. 1997;7:1595–1599.
20. Mohamed BM, Sharp JH. Kinetics of formation of $Ca_{12}Al_{14}O_{33}$ (dodecacalcium heptaaluminate). Calcium Aluminate Cements 2001, Proceedings of the International Conference on Calcium Aluminate Cements, Edinburgh, UK; 2001;65–76.
21. Jander W. Reaction in the solid state at high temperatures. I. Rate of reaction for an endothermic change. *Z Anorg Allgen Chem*. 1927;163:1–30.
22. Ginstling AM, Brownshtein BL. Concerning the diffusion kinetics of reactions in spherical particles. *J Appl Chem USSR*. 1950;23:1327–1338.
23. Carter RE. Kinetic model for solid state reaction. *J Chem Phys*. 1961;34:2010–2015.
24. Carter RE. Addendum: Kinetic model for solid state reaction. *J Chem Phys*. 1961;35:1137–1138.
25. Valensi G. Kinetics of oxidation of metallic spherules and powders. *C R Acad Sci*. 1936;202:309–312.
26. Chung HF, Smith DK. Industrial Applications of X-ray Diffraction. New York:Marcel Dekker; 2000.
27. Chen GH. Mechanical activation of calcium aluminate formation from $CaCO_3$–Al_2O_3 mixtures. *J Alloys Compd*. 2006;416:279–283.
28. Djuric M, Ranogajee J. Advances in Cement Technology: Chemistry, Manufacture and Testing. 2nd Edition. New Delhi:Tech Books International; 2002.
29. Jang SW, Lee HY, Lee SM, Lee SW, Shim KB. Mechanical activation effect on the transition of gibbsite to α-alumina. *J Mater Sci Lett*. 2000;19:507–510.
30. Jerebtsov DA, Mikhailov GG. Phase diagram of CaO–Al_2O_3 system. *Ceram Int*. 2001;27:25–28.
31. Doraiswami LK, Sharma MM. Gas–Solid Noncatalytic Reactions: Analysis and Modeling in Heterogeneous Reactions. New York: Wiley–Interscience; 1984;I:449A–479A.
32. Chibwana C, Moys MH. Radial mixing of particles in a dry batch ball mill. *Powder Technol*. 2006;163:139–144.
33. Woodman RH, Klotz BR, Dowding RJ. Evaluation of dry ball-milling technique as a method for mixing boron carbide and carbon nanotube powders. *Ceram Int*. 2005;31:765–768.
34. Jadambaa T, Kenneth JDM, Tsedev J, Banzer N, Budjav O, Mark ES, Paul A. Effect of mechanical treatment on the synthesis of calcium dialuminate. *J Mater Chem*. 2000;10:1019–1023.
35. Boldyrev VV. Mechanochemistry and mechanical activation of solids. *Solid State Ionics*. 1993;63/65:537–543.
36. Gulgun MA, Popoola OO, Kriven WM. Chemical synthesis and characterization of calcium aluminate powders. *J Am CERM Soc*. 1994;77:531–539.
37. Hao YJ, Tanaka T. Prediction of the diffusing component(s) in a solid–solid reaction system. *Solid State Ionics*. 1990;38:213–216.
38. Mchedlov-Petrosyan OP, Baubushkin VI. Thermodynamic investigation of the solid-state reactions in silicate systems. *Silikattechnik*. 1958;9:209–212.

Manuscript received July 1, 2006, and revision received Nov. 12, 2006.